



Visible-light-sensitive two-step overall water-splitting based on band structure control of titanium dioxide



Satoshi Tanigawa^a, Hiroshi Irie^{b,c,*}

^a Special Doctoral Program for Green Energy Conversion Science and Technology, Interdisciplinary Graduate School of Medicine and Engineering, University of Yamanashi, 4-3-11 Takeda, Kofu, Yamanashi 400 8511, Japan

^b Clean Energy Research Center, University of Yamanashi, 4-3-11 Takeda, Kofu, Yamanashi 400 8511, Japan

^c Japan Science and Technology Agency, CREST, 5 Sanbancho, Chiyoda-ku, Tokyo 102 0075, Japan

ARTICLE INFO

Article history:

Received 20 April 2015

Received in revised form 4 June 2015

Accepted 5 June 2015

Available online 9 June 2015

Keywords:

Titanium dioxide

Visible light

Overall water-splitting

Two-step excitation

ABSTRACT

Visible light-induced two-step overall water splitting was achieved by combining two types of photocatalysts, which were prepared by introducing foreign elements into titanium dioxide (TiO₂) with a controlled electronic band structure. Rutile and anatase TiO₂ were doped with chromium and tantalum to introduce visible-light sensitivity. Under irradiation with only visible light from a 420-nm LED lamp, the simultaneous liberation of hydrogen and oxygen with a molar ratio of ~2:1 was achieved with these two types of TiO₂-based photocatalysts in the presence of iodate ion/iodide ion as a redox mediator.

© 2015 Elsevier B.V. All rights reserved.

1. Introduction

Various photocatalytic materials have been evaluated for water splitting activity because the generated hydrogen (H₂) represents a clean and renewable fuel source [1–4]. Among examined materials, titanium dioxide (TiO₂), with which Fujishima and Honda first demonstrated photoinduced water-splitting [1], is the most promising photocatalyst due to its abundance, nontoxicity, thermal stability and high resistance against photo-corrosion. Despite these advantageous properties, TiO₂ is only sensitive to ultraviolet (UV) light and therefore requires modification for the utilization of visible light. To this end, numerous studies have examined the effects of doping foreign elements into TiO₂ on visible-light induced water-splitting [5–7]. Although doped TiO₂ is able to generate either H₂ or oxygen (O₂) in the presence of sacrificial agents following irradiation with visible light (half reaction of water-splitting), the simultaneous generation of H₂ and O₂ from water in stoichiometric amounts (overall water-splitting) has not been achieved to date.

Several photocatalysts are capable of overall water-splitting under visible-light irradiation when combined with an appropriate cocatalyst and include gallium nitride (GaN)-zinc oxide (ZnO) solid-solution [4,8–10], zinc-germanium oxynitride

((Zn_{1.44}Ge)(N₂O_{0.44})) [11], bismuth-yttrium-tungsten ternary oxide (BiYWO₆) [12], niobium-substituted silver-tantalum oxide (AgTa_{0.7}Nb_{0.3}O₃) [13], and nano-particulate CoO [14]. Combined systems consisting of two specific photocatalysts for H₂ and O₂ production and a suitable redox couple can also function as visible-light sensitive photocatalysts for overall water-splitting (two-step overall water-splitting or Z-scheme overall water-splitting) [15–17]. Recently, our group [18] and Maeda et al. [19] successfully synthesized a combined system consisting of only one mother material, strontium titanate (SrTiO₃)-based and tantalum oxynitride (TaON)-based photocatalysts, respectively. Based on the activities of these systems, it is conceivable that visible-light-sensitive two-step overall water-splitting systems could be constructed by combining only TiO₂-based materials doped with appropriate metal ions. Based on evidence in the literature, chromium (Cr) 3d forms an isolated band in the forbidden band above the valence band (VB) and below the conduction band (CB) of anatase and rutile TiO₂, respectively when Cr³⁺ is doped at a Ti⁴⁺ site [20,21]. Thus, Cr-doped anatase and rutile TiO₂ are expected to function as the H₂- and O₂-production photocatalysts, respectively.

Here, tantalum ion (Ta⁵⁺) was utilized as a counter dopant to Cr³⁺ at Ti⁴⁺ sites of anatase and rutile TiO₂ to maintain charge neutrality. Using this approach to combine Cr- and Ta-codoped TiO₂ photocatalysts in both the anatase and rutile forms, we achieved two-step overall water splitting under visible-light irradiation.

* Corresponding author. Fax: +81 55 220 8092.

E-mail address: hirie@yamanashi.ac.jp (H. Irie).

2. Experimental

2.1. Preparation of TiO₂-based photocatalysts

Cr/Ta-codoped anatase TiO₂ (Cr,Ta-TiO₂(A)) as a H₂-evolution photocatalyst was prepared by a hydrothermal synthesis method using commercial Ti(SO₄)₂ (24.0% purity, 1.92×10^{-2} mol; Kanto Kagaku), CrCl₃·6H₂O (93.0%, 4.00×10^{-4} mol; Kanto Kagaku), and TaCl₅ (4.00×10^{-4} mol; Kanto Kagaku) as starting materials. For the preparation of Cr/Ta-codoped rutile TiO₂ (Cr,Ta-TiO₂(R)) as an O₂-evolution photocatalyst, Ti(SO₄)₂ (1.96×10^{-2} mol), CrCl₃·6H₂O (1.80×10^{-4} mol), and TaCl₅ (1.80×10^{-4} mol) were utilized as the starting materials. The starting materials for the forms of TiO₂ were mixed and stirred in distilled water for 30 min using a magnetic stirrer. The solutions were treated hydrothermally in an autoclave at 140 °C for 12 h, and the resulting mixtures were washed with sufficient distilled water, collected by centrifugation, and dried at 80 °C overnight. The dried mixtures were calcined at 600 °C for 12 h for the anatase form and 900 °C for 24 h for the rutile form, and were then thoroughly ground using a mortar and pestle. As references, non-doped anatase (TiO₂(A)) and rutile (TiO₂(R)) were prepared under identical conditions using only Ti(SO₄)₂.

The deposition of platinum (Pt) co-catalyst onto the synthesized Cr,Ta-TiO₂(A) and Cr,Ta-TiO₂(R) photocatalysts was performed by a photo-deposition method. Briefly, 0.5 g of Cr,Ta-TiO₂(A) or Cr,Ta-TiO₂(R) powder was first dispersed in 100 mL methanol solution (20 vol%) as a hole scavenger. The amount of H₂PtCl₆·6H₂O (98.5% purity; Kanto Kagaku) as the source of Pt needed to give a weight fraction of Pt relative to either Cr,Ta-TiO₂(A) or Cr,Ta-TiO₂(R) of 1×10^{-3} was calculated and then added to the aqueous suspensions of each dispersed photocatalyst. The suspensions were then sufficiently deaerated using liquid nitrogen (N₂). While deaerating the suspensions, a xenon (Xe) lamp (LA-251 Xe; Hayashi Tokei) equipped with an optical filter (Y-44, Hoya) was employed for light irradiation of the suspension for 4 h. The suspension was then centrifuged, washed with distilled water, and the resulting residues were dried at 80 °C overnight. The residues were ground into a fine powder using an agate mortar to obtain the Pt-deposited Cr,Ta-TiO₂(A) (Pt/Cr,Ta-TiO₂(A)) and Cr,Ta-TiO₂(R) (Pt/Cr,Ta-TiO₂(R)) photocatalyst powders. Pt deposition on TiO₂(A) (Pt/TiO₂(A)) and TiO₂(R) (Pt/TiO₂(R)) was also performed by the same procedure, except the Xe lamp was used without an optical filter.

2.2. Characterizations

The crystal structures of the prepared powders were examined by X-ray diffraction (XRD) using a PW-1700 system (Panalytical). UV–vis absorption spectra were obtained by the diffuse reflection method using a V-650 (JASCO) spectrometer. Quantitative analyses were performed by X-ray fluorescence (XRF) using a ZSX-P1 Primus II system (Rigaku).

2.3. Photocatalytic water-splitting tests

Two types of photocatalytic water-splitting tests were performed in a gas-closed-circulation system, which was filled with argon gas (50 kPa) after deaeration. The amounts of evolved H₂ and O₂ were monitored using an online gas chromatograph (GC-8A; Shimadzu). Each time we performed the water-splitting experiments, a different amount of N₂ was detected. In addition, we repeatedly deaerated this system to a final pressure of 2.5 Pa and then introduced argon gas into the system in the same way. For these reasons, we considered that the detection of N₂ originated from the intruded air from outside, and the effect of residual O₂ (and N₂) in water was possibly excluded [13,18]. Thus, if N₂ was

detected, the O₂ amount was calculated using the following equation: $O_2 = \text{obs. } O_2 - (\text{obs. } N_2 / 0.78) \times 0.21$.

(1) Half reactions of water-splitting: H₂ and O₂ evolution was monitored in the presence of Pt/Cr,Ta-TiO₂(A) or Pt/Cr,Ta-TiO₂(R) (60 mg each) with the aid of iodide ion (I[−]) (sodium iodide (NaI), 99.5% purity, 0.01 mol/L Kanto Kagaku) or iodate ion (IO₃[−]) (sodium iodate (NaIO₃), 99.5% purity, 0.01 mol/L; Kanto Kagaku), respectively, as a sacrificial agent. The examinations were conducted in 10 mL of solution, without adjusting the pH, with constant stirring using a magnetic stirrer and under irradiation with visible light generated from a light-emitting diode (LED) lamp with a wavelength of 420 nm (420-nm LED, LEDH60-420, Hamamatsu Photonics).

(2) Two-step overall water splitting: Photocatalytic overall water-splitting experiments were conducted by adding the sample powders (Pt/Cr,Ta-TiO₂(A): 90 mg, Pt/Cr,Ta-TiO₂(R): 10 mg) to 10 mL I[−]/IO₃[−] solutions (I[−]: 8 mL, IO₃[−]: 2 mL) as redox mediators. The suspension was constantly stirred using a magnetic stirrer and the pH was not adjusted. The 420-nm LED light was used for light irradiation. As references, the water-splitting experiments were performed under the identical conditions with 90 mg of Cr,Ta-TiO₂(A) in place of Pt/Cr,Ta-TiO₂(A) and 10 mg of Pt/Cr,Ta-TiO₂(R) as well as with 90 mg of Pt/Cr,Ta-TiO₂(A) and 10 mg of Pt/TiO₂(R) in place of Pt/Cr,Ta-TiO₂(R), in addition to 90 mg of Pt/TiO₂(A) and 10 mg of Pt/TiO₂(R).

2.4. Isotope labeled-water splitting

Photocatalytic overall water-splitting tests were also conducted with the Pt/Cr,Ta-TiO₂(A) and Pt/Cr,Ta-TiO₂(R) powders suspended in 10 mL of I[−]/IO₃[−] solution containing 30% isotopic water (H₂¹⁸O, purity, 97 atom% ¹⁸O; Sigma-Aldrich,) under the same conditions as above. Evolved gas was detected by a gas chromatograph mass spectrometer (GCMS, GCMS-QP 2010 Ultra, Shimadzu) operated in selective-ion mode to monitor for 28 (N₂), 32 (¹⁶O¹⁶O), 34 (¹⁶O¹⁸O), and 36 (¹⁸O¹⁸O) ions. Spectra were measured under the same conditions used for two-step overall water splitting tests. Natural isotopic compositions of ¹⁶O, ¹⁷O, and ¹⁸O are 99.757, 0.038, and 0.205 atm%, respectively [22]. Then, the compositions of ³²O₂ (¹⁶O¹⁶O), ³⁴O₂ (¹⁶O¹⁸O, ¹⁷O¹⁷O), and ³⁶O₂ (¹⁸O¹⁸O) in the atmospheric condition are calculated to be 99.515, 0.409, and 0.000420 atm%, respectively. We plotted the calculated ¹⁶O¹⁸O and ¹⁸O¹⁸O values using the following equation provided that the ¹⁴N¹⁴N was observed as the result of air contamination from outside as mentioned above: $^{16}O^{18}O = \text{obs. } ^{16}O^{18}O - (\text{obs. } N_2 \times 0.21 / 0.78) \times 0.409 \times 10^{-2}$, and $^{18}O^{18}O = \text{obs. } ^{18}O^{18}O - (\text{obs. } N_2 \times 0.21 / 0.78) \times 0.000420 \times 10^{-2}$ (in fact, ¹⁸O¹⁸O was considered to be equal to obs. ¹⁸O¹⁸O due to the extremely small value of 0.000420×10^{-2}).

3. Results and discussion

3.1. Characterization of the prepared photocatalysts

Elemental analyses by XRF indicated that the molar ratios of Ti: Cr: Ta in Pt/Cr,Ta-TiO₂(A) were 0.982: 0.004: 0.014 and those of Ti: Cr: Ta in Pt/Cr,Ta-TiO₂(R) were 0.992: 0.002: 0.006. Notably, these molar ratios were not consistent with the starting ratios used in the preparation of the photocatalysts. This discrepancy was attributed to differences in the solubility of Ti, Cr and Ta in aqueous solution under hydrothermal conditions. The analyses also indicated that the molar fractions of Pt relative to Cr,Ta-TiO₂(A) and Cr,Ta-TiO₂(R) were 9×10^{-4} and 5×10^{-4} , respectively. Cr,Ta-TiO₂(A) and Cr,Ta-TiO₂(R) were confirmed to have a single phase of anatase and rutile TiO₂, respectively, in the obtained XRD spectra (Fig. 1a). In addition, the XRD peaks of Cr,Ta-TiO₂(A) and Cr,Ta-TiO₂(R) were shifted

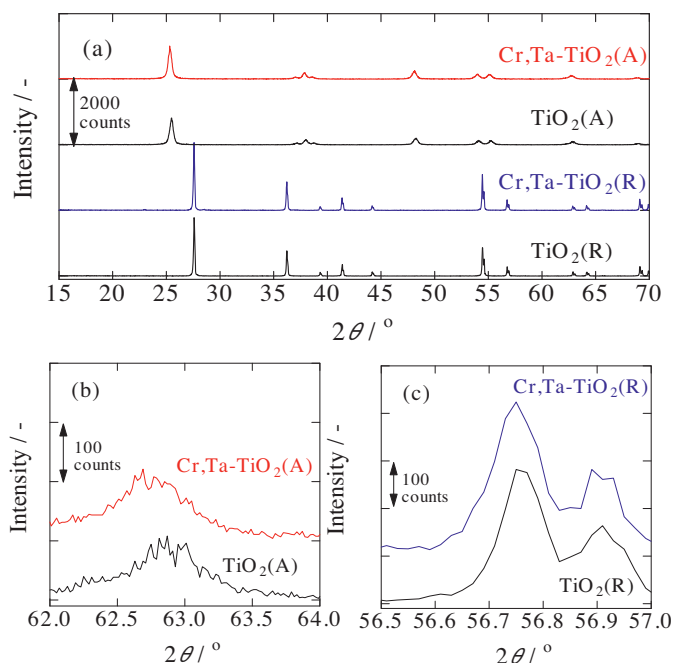


Fig. 1. XRD patterns of prepared $\text{TiO}_2(\text{A})$, $\text{Cr,Ta-TiO}_2(\text{A})$, $\text{TiO}_2(\text{R})$, and $\text{Cr,Ta-TiO}_2(\text{R})$ powders (a)–(c) are enlargements of (a).

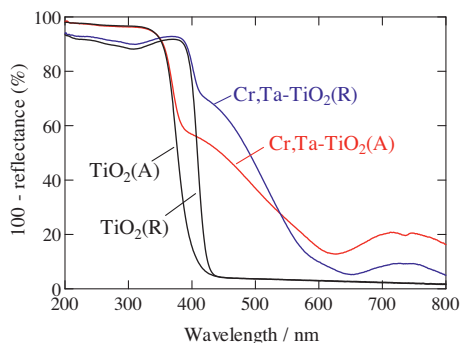


Fig. 2. UV-visible absorption spectra of $\text{TiO}_2(\text{A})$, $\text{Cr,Ta-TiO}_2(\text{A})$, $\text{TiO}_2(\text{R})$, and $\text{Cr,Ta-TiO}_2(\text{R})$.

to a lower 2θ angle compared to non-doped $\text{TiO}_2(\text{A})$ and $\text{TiO}_2(\text{R})$ (Figs. 1b and 1c). These results are reasonable when one considers that the effective ionic radii of Ti^{4+} , Cr^{3+} , and Ta^{5+} (six-coordination) are 0.0605, 0.0615, and 0.064 nm, respectively [23]. Thus, in both the anatase and rutile forms of the TiO_2 photocatalysts, Cr and Ta ions were likely incorporated at Ti sites.

The UV-visible absorption spectra of $\text{TiO}_2(\text{A})$, $\text{Cr,Ta-TiO}_2(\text{A})$, $\text{TiO}_2(\text{R})$, and $\text{Cr,Ta-TiO}_2(\text{R})$ were measured using a diffuse reflection method (Fig. 2). In the spectra of both $\text{Cr,Ta-TiO}_2(\text{A})$ and $\text{Cr,Ta-TiO}_2(\text{R})$, an absorption shoulder in the visible-light region and a negligible shift of the absorption edges were observed compared to those of $\text{TiO}_2(\text{A})$ and $\text{TiO}_2(\text{R})$. These findings indicate that the bandgaps of $\text{Cr,Ta-TiO}_2(\text{A})$ and $\text{Cr,Ta-TiO}_2(\text{R})$ did not markedly differ from those of $\text{TiO}_2(\text{A})$ and $\text{TiO}_2(\text{R})$, respectively.

3.2. Half reactions of water-splitting

We next examined the evolution of H_2 and O_2 by $\text{Pt/Cr,Ta-TiO}_2(\text{A})$ and $\text{Pt/Cr,Ta-TiO}_2(\text{R})$ in the presence of I^- and IO_3^- as sacrificial agents, respectively, and under irradiation with visible light ($> 420 \text{ nm}$). As shown in Fig. 3, H_2 evolution by $\text{Pt/Cr,Ta-TiO}_2(\text{A})$ was only detected for in the presence of I^- , and was not

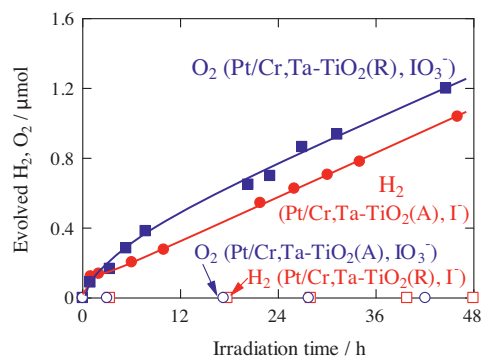


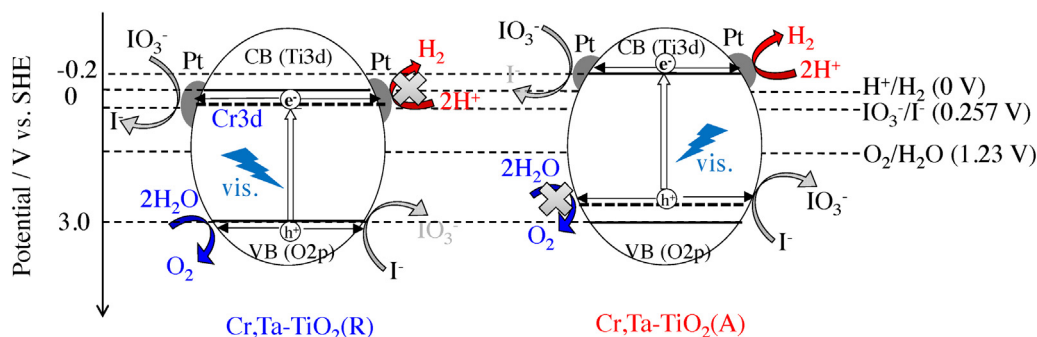
Fig. 3. Time courses of O_2 evolution resulting from the half water-reaction by $\text{Pt/Cr,Ta-TiO}_2(\text{R})$ photocatalyst irradiated with visible light (420-nm LED) in the presence of IO_3^- as a sacrificial agent. H_2 evolution was also monitored, but H_2 was not detected. Time courses of H_2 evolution by $\text{Pt/Cr,Ta-TiO}_2(\text{A})$ photocatalyst irradiated with visible light (420-nm LED) in the presence of I^- as a sacrificial agent. O_2 evolution was also measured, but was not detected.

observed in the system with $\text{Pt/Cr,Ta-TiO}_2(\text{R})$. In contrast, O_2 evolution was only detected for $\text{Pt/Cr,Ta-TiO}_2(\text{R})$ in the presence of IO_3^- , and did not proceed for $\text{Pt/Cr,Ta-TiO}_2(\text{A})$. Thus, we could confidently conclude that the introduced Cr 3d orbital in $\text{Cr,Ta-TiO}_2(\text{A})$ was responsible for the oxidation of I^- and was not involved in O_2 evolution, whereas the CB of $\text{Cr,Ta-TiO}_2(\text{A})$ was responsible for H_2 evolution under irradiation with visible light. In contrast, the introduced Cr 3d orbital in $\text{Cr,Ta-TiO}_2(\text{R})$ was responsible for the reduction of IO_3^- and was not involved in the evolution of H_2 , whereas the VB of $\text{Cr,Ta-TiO}_2(\text{R})$ was responsible for O_2 evolution under irradiation with visible light. From these experimental results, in combination with the UV-visible absorption spectra, we confirmed that Cr 3d forms an isolated band above the VB in $\text{Cr,Ta-TiO}_2(\text{A})$ and below the CB of $\text{Cr,Ta-TiO}_2(\text{R})$ (Scheme 1). Although the potential of Cr 3d orbital in $\text{Cr,Ta-TiO}_2(\text{A})$ is lower than the $\text{O}_2/\text{H}_2\text{O}$ potential (1.23 V vs. SHE), O_2 evolution was not observed. This is plausible when we consider the overpotential for O_2 evolution. To reduce the overpotential, intensive studies to investigate a cocatalyst that can reduce the overpotential have been performed by mimicking O_2 -evolving centers in photosystem II in artificial photosynthetic systems [24–26]. If such a cocatalyst is grafted on the surface of $\text{Cr,Ta-TiO}_2(\text{A})$, it would be able to oxidize water to produce O_2 .

3.3. Two-step overall water splitting

We examined water splitting by the $\text{Pt/Cr,Ta-TiO}_2(\text{A})$ and $\text{Pt/Cr,Ta-TiO}_2(\text{R})$ photocatalysts under visible-light irradiation (420-nm LED) for 500 h in the presence of IO_3^-/I^- as a redox mediator (Fig. 4). As shown in Fig. 4a, the levels of H_2 and O_2 increased in a linear manner with increasing irradiation time and repeated evacuations of the system. Notably, H_2 to O_2 were evolved at similar levels in nearly stoichiometric (~ 2 –1) amounts during each irradiation cycle. These results demonstrate that overall water-splitting was achieved in this system.

In contrast to the combination of bare $\text{Cr,Ta-TiO}_2(\text{A})$ and $\text{Pt/Cr,Ta-TiO}_2(\text{R})$, and IO_3^-/I^- as a redox mediator in the system, trace amounts of O_2 were produced under irradiation with visible light (420-nm LED), but H_2 was not detected (Fig. 4b). This result indicates that Pt on $\text{Cr,Ta-TiO}_2(\text{A})$ functions as the site of H_2 evolution. As determined by XRF analysis, the $\text{Pt/Cr,Ta-TiO}_2(\text{A})$ sample contained Pt at a molar percentage of 9×10^{-4} (0.09 mol%). Therefore, because a total of 90 mg of the $\text{Pt/Cr,Ta-TiO}_2(\text{A})$ sample was used in the water-splitting experiment, the amount of Pt was $0.98 \mu\text{mol}$. As the total amount of H_2 generated during the 500-h experiment was $1.12 \mu\text{mol}$, we estimated that the turnover



Scheme 1. Schematic illustrations of the half-reaction of water splitting, O_2 evolution over Pt/Cr,Ta-TiO₂(R) photocatalyst irradiated with visible light (420-nm LED) in the presence of the sacrificial agent IO_3^- , and H_2 evolution over Pt/Cr,Ta-TiO₂(A) photocatalyst irradiated with visible light (420-nm LED) in the presence of I^- as a sacrificial agent.

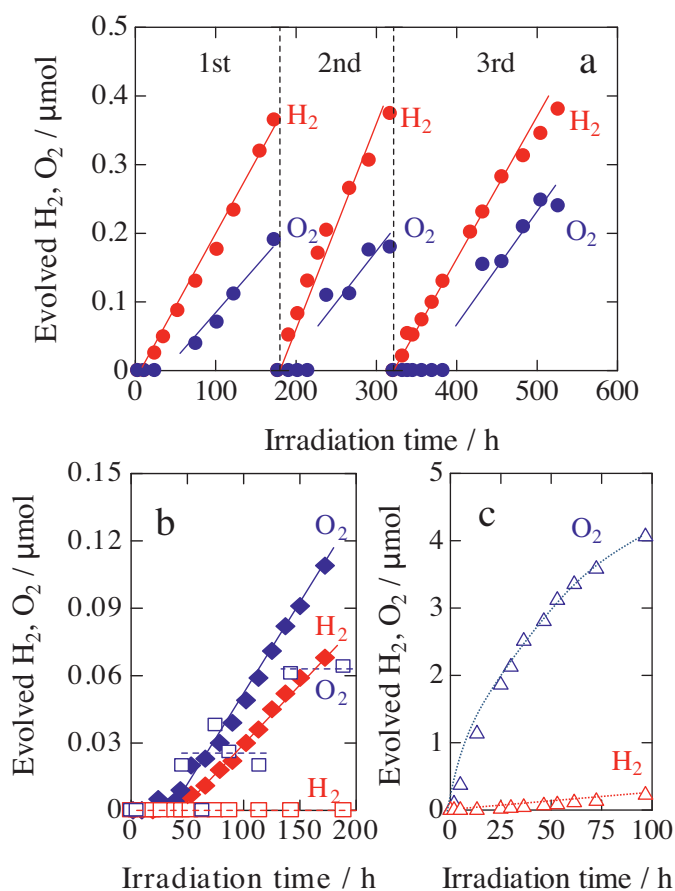
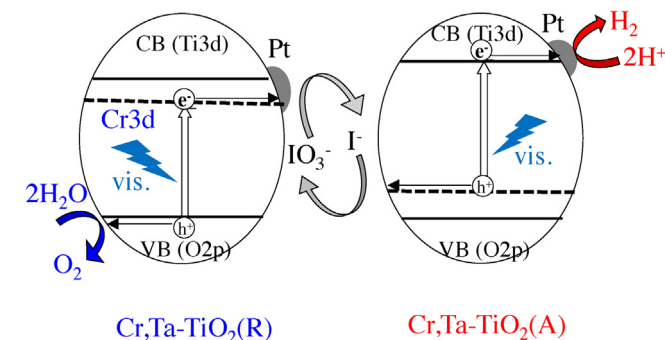


Fig. 4. (a) Time courses of H_2 and O_2 evolution resulting from photocatalytic water-splitting by Pt/Cr,Ta-TiO₂(A) and Pt/Cr,Ta-TiO₂(R) under irradiation with visible light (420-nm LED). The reaction was allowed to proceed for 500 h with twice evacuations of the system. (b) The time courses of H_2 and O_2 evolution for Cr,Ta-TiO₂(A) and Pt/Cr,Ta-TiO₂(R) photocatalysts (open square) and for Pt/Cr,Ta-TiO₂(A) and Pt/TiO₂(R) photocatalysts (closed rhombus) irradiated with visible light (420-nm LED). (c) H_2 and O_2 evolution by Pt/TiO₂(A) and Pt/TiO₂(R) photocatalysts irradiated with visible light (420-nm LED).

number, the ratio of total amount of produced to H_2 to that of Pt co-catalyst, was 1.14, which exceeded 1, indicating that this reaction proceeded catalytically.

It should be noted that in the system with Pt/TiO₂(A) and Pt/TiO₂(R) under identical conditions as those used for the above water-splitting experiments, a large amount of O_2 was produced due to the half-reaction of Pt/TiO₂(R) in the presence of IO_3^- acting as the sacrificial agent, resulting in a large deviation from the stoichiometric ratio of H_2 and O_2 evolution (Fig. 4c). Moreover, in the system with Pt/Cr,Ta-TiO₂(A) and Pt/TiO₂(R) under identical conditions, simultaneous H_2 and O_2 were evolved; however they were extremely small amounts at the non-stoichiometric ratio (Fig. 4b). Thus, the introduced Cr 3d orbitals in the Cr,Ta-TiO₂(A) and Cr,Ta-TiO₂(R) photocatalysts play an important role in generating H_2 and O_2 in stoichiometric amounts.



Scheme 2. Schematic illustrations of spontaneous H_2 and O_2 evolution over Pt/Cr,Ta-TiO₂(A) and Pt/Cr,Ta-TiO₂(R) photocatalysts irradiated with visible light (420-nm LED) in the presence of IO_3^-/I^- redox mediator.

chiometric ratio of H_2 and O_2 evolution (Fig. 4c). Moreover, in the system with Pt/Cr,Ta-TiO₂(A) and Pt/TiO₂(R) under identical conditions, simultaneous H_2 and O_2 were evolved; however they were extremely small amounts at the non-stoichiometric ratio (Fig. 4b). Thus, the introduced Cr 3d orbitals in the Cr,Ta-TiO₂(A) and Cr,Ta-TiO₂(R) photocatalysts play an important role in generating H_2 and O_2 in stoichiometric amounts.

Taking Scheme 1 and the results presented in Fig. 4a and b into consideration, we propose a probable mechanism for overall water splitting by Pt/Cr,Ta-TiO₂(A) and Pt/Cr,Ta-TiO₂(R), as schematically illustrated in Scheme 2. In this model, visible light-excited electrons in the CB of Cr,Ta-TiO₂(A) are thought to reduce H_2O and generate H_2 , whereas holes in the VB of Cr,Ta-TiO₂(R), which oxidize H_2O to produce O_2 . In addition, visible-light-excited holes in the isolated Cr 3d state of Cr,Ta-TiO₂(A) and electrons in the isolated Cr 3d state contribute to the turn-over of I^- to IO_3^- and IO_3^- to I^- , respectively.

3.4. Isotope labeled-water splitting

To confirm the production of O_2 from water by this system under visible-light irradiation (420-nm LED), we examined water splitting using water containing 30% H_2^{18}O (Fig. 5). As N_2 was unexpectedly detected, $^{16}\text{O}^{16}\text{O}$ was not included in the analysis, which was therefore limited to $^{16}\text{O}^{18}\text{O}$ and $^{18}\text{O}^{18}\text{O}$. We could repeatedly detect $^{16}\text{O}^{18}\text{O}$ and $^{18}\text{O}^{18}\text{O}$ following irradiation of the system with 420-nm light, but did not detect $^{18}\text{O}^{18}\text{O}$ under dark conditions. Although a small amount of $^{16}\text{O}^{18}\text{O}$ was observed under dark conditions, however the detected peak area was so small, causing the poor signal/noise (S/N) ratio. In addition, we couldn't have tendency to increase with increasing dark storage time. At the moment, we cannot confidently conclude whether $^{16}\text{O}^{18}\text{O}$ indeed formed or not. The $^{16}\text{O}^{18}\text{O}$ amount under dark conditions was much smaller than

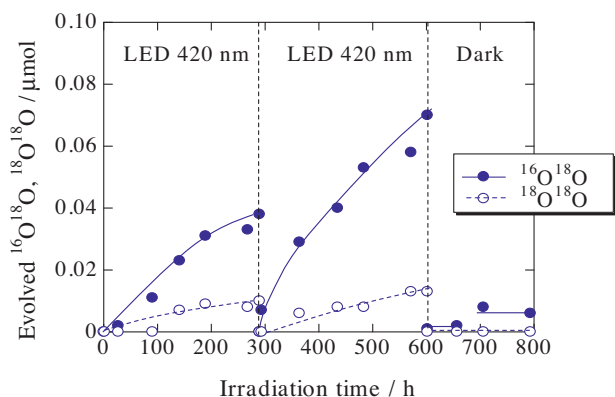


Fig. 5. Time courses of $^{16}\text{O}^{18}\text{O}$ and $^{18}\text{O}^{18}\text{O}$ evolution from water containing 30% H_2^{18}O by Pt/Cr,Ta- TiO_2 (A) and Pt/Cr,Ta- TiO_2 (R) photocatalysts irradiated with visible light (420-nm LED). The reaction was allowed to proceed for 600 h with once evacuation. After a final evacuation of the system, the amount of $^{16}\text{O}^{18}\text{O}$ and $^{18}\text{O}^{18}\text{O}$ produced under dark conditions was also measured.

that detected in the system irradiated with 420-nm light. More importantly, $^{18}\text{O}^{18}\text{O}$ was detected under 420-nm light, whereas was not detected at all under dark conditions. Thus, it was confirmed that O_2 was liberated from water by the photocatalytic system under visible-light irradiation at 420 nm.

4. Conclusions

We established a two-step overall water-splitting system that is sensitive to visible light by utilizing two types of TiO_2 -based photocatalysts that simultaneously evolve H_2 and O_2 at a molar ratio of $\sim 2:1$ in the presence of IO_3^-/I^- . However, because the evolution rates were not high, it is necessary to further enhance the visible-light sensitivity of these TiO_2 -based materials by optimizing the concentrations and types of dopants or by preparing deficient-free doped TiO_2 . We have recently developed a solid-state two-step overall water-splitting photocatalyst, in which the H_2 - and O_2 -evolution photocatalysts were connected via silver [27]. In this system, distilled water could be split without a redox mediator. The construction of solid-state systems using TiO_2 -based photocatalysts may be advantageous for industrial and practical applications, as no chemicals are required as sacrificial agents.

Acknowledgements

We express gratitude to Mr. G. Newton for the careful reading of the manuscript.

References

- [1] A. Fujishima, K. Honda, *Nature* 238 (1972) 37–38.
- [2] J. Sato, N. Saito, H. Nishiyama, Y. Inoue, *J. Phys. Chem. B* 105 (2001) 6061–6063.
- [3] H. Kato, K. Asakura, A. Kudo, *J. Am. Chem. Soc.* 125 (2003) 3082–3089.
- [4] K. Maeda, K. Teramura, D. Lu, T. Takata, N. Saito, K. Inoue, Y. Domen, *Nature* 440 (2006) 295.
- [5] H. Kato, A. Kudo, *J. Phys. Chem. B* 106 (2002) 5029–5034.
- [6] R. Niishiro, R. Kenta, H. Kato, W.-J. Chun, K. Asakura, A. Kudo, *J. Phys. Chem. C* 111 (2007) 17420–17426.
- [7] L. Li, J. Yan, T. Wang, Z.-J. Zhao, J. Zhang, J. Gong, N. Guan, *Nature Commun.* 6 (2015) 5881/1–5881/10.
- [8] K. Maeda, T. Takata, M. Hara, N. Saito, Y. Inoue, H. Kobayashi, K. Domen, *J. Am. Chem. Soc.* 127 (2005) 8286–8287.
- [9] K. Maeda, K. Teramura, T. Takata, M. Hara, N. Saito, K. Toda, Y. Inoue, H. Kobayashi, K. Domen, *J. Phys. Chem. B* 109 (2005) 20504–20510.
- [10] K. Teramura, K. Maeda, T. Saito, T. Takata, N. Saito, Y. Inoue, K. Domen, *J. Phys. Chem. B* 109 (2005) 21915–21921.
- [11] Y. Lee, H. Terashima, Y. Shimodaira, K. Teramura, M. Hara, H. Kobayashi, K. Domen, M. Yashima, *J. Phys. Chem. C* 111 (2007) 1042–1048.
- [12] H. Liu, J. Yuan, W. Shangguan, Y. Teraoka, *J. Phys. Chem. C* 112 (2008) 8521–8523.
- [13] N. Lei, M. Tanabe, H. Irie, *Chem. Commun.* 49 (2013) 10094–10096.
- [14] L. Liao, Q. Zhang, Z. Su, Z. Zhao, Y. Wang, Y. Li, X. Lu, D. Wei, G. Feng, Q. Yu, X. Cai, J. Zhao, Z. Ren, H. Fang, F.R. -Hernandez, S. Baldelli, J. Bao, *Nature Nanotech.* 9 (2014) 69–73.
- [15] K. Sayama, K. Mukasa, R. Abe, Y. Abe, H. Arakjawa, *J. Photo. Photo. A* 148 (2002) 71–77.
- [16] H. Kato, Y. Sasaki, A. Iwase, A. Kudo, *Bull. Chem. Soc. Jpn.* 80 (2007) 2457–2464.
- [17] A. Kudo, *Int. J. Hydrogen Energy* 32 (2007) 2673–2678.
- [18] S. Hara, M. Yoshimizu, S. Tanigawa, L. Ni, B. Ohtani, H. Irie, *J. Phys. Chem. C* 116 (2012) 17458–17463.
- [19] K. Maeda, R. Abe, K. Domen, *J. Phys. Chem. Lett.* 115 (2011) 3057–3064.
- [20] T. Umehayashi, T. Yamaki, H. Itoh, K. Asai, *J. Phys. Chem. Solids* 63 (2012) 1909–1920.
- [21] C. Di Valentin, G. Pacchioni, H. Onishi, A. Kudo, *Chem. Phys. Lett.* 469 (2009) 166–171.
- [22] K.J.R. Rosman, P.D.P. Taylor, *Pure Appl. Chem.* 70 (1998) 217–235.
- [23] R.D. Shannon, C.T. Prewitt, *Acta Cryst. B* 25 (1969) 925–946.
- [24] M.W. Kanan, Y. Surendranath, D.G. Nocera, *Chem. Soc. Rev.* 38 (2009) 109–114.
- [25] J. Suntivich, K.J. May, H.A. Gasteiger, J.B. Goodenough, Y.S. -Horn, *Science* 334 (2011) 1383–1385.
- [26] T. Takashima, K. Hashimoto, R. Nakamura, *J. Am. Chem. Soc.* 134 (2012) 18153–18156.
- [27] R. Kobayashi, S. Tanigawa, T. Takashima, B. Ohtani, H. Irie, *J. Phys. Chem. C* 118 (2014) 22450–22456.